Exploiting Block Sparsity for Joint Mitigation of Asynchronous NBI and IN in Hybrid Powerline-Wireless Communications

Mohamed Mokhtar*, Waheed U. Bajwa†, Mahmoud Elgenedy*, and Naofal Al-Dhahir*
*University of Texas at Dallas, USA, Emails: {m.mokhtar, mahmoud.elgenedy, aldhahir}@utdallas.edu
†Rutgers, The State University of New Jersey, Email: waheed.bajwa@rutgers.edu

***Abstract*—Transmission of the same information signal simultaneously over multiple physical layers, such as powerline and unlicensed wireless communication networks, results in higher reliability and/or enhances the coverage range compared to using a single physical layer due to diversity gains. However, each physical layer suffers from its own distinct impairments that can severely degrade performance. Unlicensed wireless communications suffers from narrow-band interference (NBI) while powerline communications (PLC) is impaired by impulsive noise (IN). With orthogonal frequency division multiplexing used for both communication systems, these two impairments, if not mitigated, can severely degrade performance. This paper proposes an approach for efficient joint estimation and mitigation of the NBI and IN signals in hybrid wireless and PLC systems. The proposed approach exploits the inherent sparse structures of the NBI and IN signals in the frequency and time domains, respectively, and is based on the compressive sensing (CS) principles. The paper also addresses the practical asynchronous NBI scenario that suffers from carrier frequency offset (CFO) with respect to the wireless received signal. In this regard, it investigates the use of time-domain windowing to enhance the NBI's sparsity and, hence, improve its subsequent estimation and mitigation. Further, the paper enhances the estimation and mitigation of NBI and IN by modeling the burstiness of both impairments as block-sparse vectors. To this end, it investigates the performance of two block-sparse CS recovery algorithms with and without prior knowledge of the bursts' boundaries. Finally, numerical experiments quantify the performance gains realized by exploiting both the burstiness and sparsity of the NBI and IN signals over exploiting sparsity alone.**

I. Introduction

Diversity reception techniques exploiting time, frequency, space, or combinations thereof, are widely used to combat the detrimental channel and interference effects [1]. To meet the ever-increasing data rate demands and further improve communication reliability, hybrid diversity receive combining based on multiple physical layers has gained increasing interest recently. Unlicensed wireless communications and powerline communications (PLC) are attractive candidates to achieve this objective due to their ubiquity [2], [3].

In-home broadband PLC standards such as IEEE P1901.1 and ITU-T G.hn [4] use orthogonal frequency division multiplexing (OFDM) and operate in the 1.8–250 MHz frequency band. In-home broadband wireless local area networks (WLAN) standards such as IEEE 802.11g/n also use OFDM and operate in the unlicensed 2.4 GHz and/or 5 GHz ISM frequency bands. To improve transmission reliability, a hybrid PLC-wireless system can simultaneously transmit OFDM symbols over both PLC and WLAN channels and jointly process their received signals to exploit independence of the two channels and interference characteristics of the two physical media. Note that while channel fading and interference in receive-diversity-based wireless systems follow the same statistical distributions on all branches, these distributions can be markedly different for the PLC and wireless branches.

WLAN signals experience narrow-band interference (NBI) from co-existing wireless communication systems sharing the same frequency band such as cordless phones and Bluetooth devices in the 2.4 GHz band [5]. Given its narrowband nature, NBI distorts the desired signal, but it occupies few OFDM sub-carriers which makes it sparse in the frequency domain. On the other hand, in-home PLC networks suffer from impulsive noise (IN) due to abrupt voltage changes caused by on-off switching of in-home appliances and power electronics devices such as silicon-controlled rectifiers, switching regulators, and brush motors [6]. These bursty impulses are limited in the time-domain compared to the desired data OFDM symbol duration. Our goal in this paper is to investigate novel approaches for joint estimation and mitigation of NBI and IN in hybrid PLC-wireless systems by exploiting their inherent sparse structures in the frequency and time domains, respectively.

In practice, the NBI is asynchronous and, hence, exhibits a frequency offset with respect to the desired signal. Therefore, the NBI energy leaks to neighboring sub-carriers and occupies a wider frequency band within the desired signal. This makes the NBI less sparse and, hence, less amenable for accurate estimation using sparse recovery algorithms. As a practical solution to this problem, we investigate the effect of applying time-domain windowing to the received signal to enhance the sparsity of NBI in the presence of CFO.

Furthermore, both NBI and IN exhibit burstiness, which makes their representations block sparse where the non-zero coefficients occur in clusters (or bursts) [7], [8]. Based on compressive sensing (CS) theory, several algorithms have been proposed to reconstruct spare or block-sparse signals from an under-determined linear model. These include l_1 minimization and greedy algorithms; see [7]–[9] and the references therein.

Considering prior works, mitigation of NBI and IN in OFDM systems was studied in [2], [3], [5], [10], [11]. But [2], [3] do not exploit the sparse structures of NBI and IN. In addition, [2] assumes frequency-flat (non-selective) PLC and wireless channels, while [3] assumes them to be deterministic. Both [5] and [10] do exploit sparsity of NBI and IN to mitigate them using CS techniques. They demonstrate that CS-based mitigation of NBI or IN outperforms traditional interference cancellation schemes. However, they do not consider joint mitigation of NBI and IN. In [11], the author exploits the block-sparse structure to estimate the IN in PLC networks. Our work differs from [11] in that we consider hybrid wireless and PLC networks and we jointly mitigate both NBI and IN.

This work is supported by NPRP grant # NPRP 6-070-2-024 from the Qatar National Research Fund (a member of Qatar Foundation). The statements made herein are solely the responsibility of the authors.

Moreover, we utilize two block-sparse recovery CS algorithm with and without knowledge of the IN and NBI bursts' boundaries. Finally, we consider multiple-output systems for each of the PLC and wireless systems unlike [11] which assumed a single output.

The work in here is an extension of our earlier work [12] that developed a novel CS-based framework for joint estimation and mitigation of NBI and IN that exploits their inherent sparsity in different domains. While our formulation in [12] accommodates multiple receive antennas and multiple PLC wires, it neither addresses the practical scenario of asynchronous NBI nor does it exploit the burstiness of the NBI and IN signals in the frequency and time domains, respectively. Our main contributions in this regard are as follows. First, we enhance the sparsity of the asynchronous NBI signal by applying time-domain windowing. Second, we exploit the NBI and IN block-sparse (bursty) structure and investigate CS recovery algorithms under different assumptions. With known bursts' boundaries, we investigate the block orthogonal matching pursuit (BOMP) algorithm [7]. In the absence of such knowledge, we investigate another CS recovery algorithm proposed in [8]. Finally, we quantify the performance gains of our proposed approaches through extensive numerical experiments.

A. Notation and paper organization

Notation: Lower- and upper-case bold letters denote vectors and matrices, respectively. $\mathbf{I}$ and $\mathbf{F}$ denote the identity and the Fast Fourier transform (FFT) matrices, respectively, while subscripts denote their sizes. The frequency-domain matrices/vectors are denoted by $\mathbf{A}_x^{(i)}$/$\mathbf{a}_x^{(i)}$, where $x \in \{W, P\}$ denotes the transmission system with W and P for wireless and PLC systems, respectively, while the superscript i indicates the i^{th} antenna or wire. The corresponding time-domain matrices/vectors are denoted by $\bar{\mathbf{A}}_x^{(i)}$/$\bar{\mathbf{a}}_x^{(i)}$. Further, $(\cdot)^H$, $(\cdot)^*$, $(\cdot)^T$, $\mathbb{E}[\cdot]$, and $|\cdot|$ denote the complex-conjugate transpose, complex-conjugate, transpose, statistical expectation and absolute-value operations, respectively. Note that $|\cdot|$ with a vector argument denotes element-wise absolute-value operation. Finally, we use the terms "burst" and "cluster" interchangeably throughout the paper to denote a block of contiguous non-zero elements in the sparse NBI and IN vectors.

Paper Organization: Our system model, assumptions for hybrid indoor PLC-wireless networks, and the problem formulation are described in Section II. CS-based approaches for joint mitigation of NBI and IN are presented in Section III. Finally, numerical experiments and concluding remarks are provided in Sections IV and V, respectively.

II. System Model

We consider single-input multiple-output (SIMO) OFDM simultaneous transmissions over PLC and wireless channels [3] (see Fig. 1). The wireless system operates in an unlicensed WLAN band and consists of a single-antenna transmitter and a receiver equipped with K antennas. The PLC receiver can process up to $\beta \in \{1, 2, 3\}$ outputs over its 3 wires. We assume that each antenna at the wireless receiver suffers from uncorrelated NBI and the 3 wires of the PLC channel experience uncorrelated IN.[1] Under these assumptions, the received signals at the k^{th}, $k \in \{1, \ldots, K\}$, antenna and the j^{th}, $j \in \{1, \ldots, \beta\}$, wire are given by

$$\bar{\mathbf{y}}_W^{(k)} = \bar{\mathbf{H}}_W^{(k)} \bar{\mathbf{x}} + \mathbf{D}_W^{(k)} \bar{\mathbf{i}}_W^{(k)} + \bar{\mathbf{n}}_W^{(k)}, \tag{1}$$

$$\bar{\mathbf{y}}_P^{(j)} = \bar{\mathbf{H}}_P^{(j)} \bar{\mathbf{x}} + \bar{\mathbf{i}}_P^{(j)} + \bar{\mathbf{n}}_P^{(j)}, \tag{2}$$

where the subscripts W and P denote the wireless and PLC systems, respectively. Here, assuming M OFDM sub-carriers, $\bar{\mathbf{H}}_W^{(k)}$ and $\bar{\mathbf{H}}_P^{(j)}$ denote $M \times M$ circulant channel matrices between the transmitter's antenna/wire and the $k^{\text{th}}/j^{\text{th}}$ receiver's antenna/wire of the wireless and PLC systems, respectively. The first columns of these matrices are $\begin{bmatrix} \bar{\mathbf{h}}_W^{(k)T} & \mathbf{0}_{1\times M-L_W} \end{bmatrix}^T$ and $\begin{bmatrix} \bar{\mathbf{h}}_P^{(j)T} & \mathbf{0}_{1\times M-L_P} \end{bmatrix}^T$, where $\bar{\mathbf{h}}_W^{(k)}$ and $\bar{\mathbf{h}}_P^{(j)}$ are the wireless and PLC channel impulse response (CIR) vectors with L_W and L_P complex taps, respectively. We assume that the wireless CIR taps are zero-mean complex Gaussian random variables, while the PLC CIR taps are log-normal distributed [2]. In addition, we assume the availability of perfect channel state information (CSI) at the wireless and PLC receivers.

Using $\mathbf{x}$ for the $M \times 1$ OFDM data symbols vector, $\bar{\mathbf{x}}$ in (1), (2) is defined as $\bar{\mathbf{x}} = \mathbf{F}_M^* \mathbf{x}$. In addition, $\bar{\mathbf{n}}_W^{(k)}$ and $\bar{\mathbf{n}}_P^{(j)}$ denote complex zero-mean circularly-symmetric additive-white-Gaussian noise (AWGN) vectors at the $k^{\text{th}}/j^{\text{th}}$ receiver's antenna/wire with variances σ_W^2 and σ_P^2, respectively. The NBI (which is sparse in the frequency domain) and the IN (which is sparse in the time-domain) vectors at each antenna/PLC wire are denoted by $\bar{\mathbf{i}}_W^{(k)}$ and $\bar{\mathbf{i}}_P^{(j)}$, respectively. Finally, the diagonal matrix $\mathbf{D}_W^{(k)} \triangleq \text{diag}\left[1,\ \exp\left(i\frac{2\pi\alpha^{(k)}}{M}\right),\ \cdots,\ \exp\left(i\frac{2\pi\alpha^{(k)}(M-1)}{M}\right)\right]$, where $i = \sqrt{-1}$ and $\alpha^{(k)}$ is the carrier frequency offset (CFO) coefficient between the NBI signal and the received signal at the wireless receiver. The CFO coefficient, denoted by $\alpha^{(k)}$, is normalized to the subcarrier spacing, assumed uniformly-distributed in the interval $[-0.5,\ 0.5]$, and may differ from one receive antenna to another.

CFO destroys the NBI orthogonality and results in energy leakage among the neighboring sub-carriers. Hence, the NBI sparsity level is reduced. To enhance the system's robustness against CFO, we use time-domain windowing methods to suppress the FFT side lobes and restore the sparsity of the NBI signal. Applying windowing to the wireless received signal and then taking the FFT of (1) and (2), we get

$$\underbrace{\mathbf{F}_M \Phi \bar{\mathbf{y}}_W^{(k)}}_{\triangleq \mathbf{y}_W^{(k)}} = \underbrace{\mathbf{F}_M \Phi \bar{\mathbf{H}}_W^{(k)} \mathbf{F}_M^*}_{\triangleq \Lambda_W^{(k)}} \mathbf{x} + \underbrace{\mathbf{F}_M \Phi \mathbf{D}_W^{(k)} \bar{\mathbf{i}}_W^{(k)}}_{\triangleq \mathbf{i}_W^{(k)}} + \underbrace{\mathbf{F}_M \Phi \bar{\mathbf{n}}_W^{(k)}}_{\triangleq \mathbf{n}_W^{(k)}}, \tag{3}$$

$$\underbrace{\mathbf{F}_M \bar{\mathbf{y}}_P^{(j)}}_{\triangleq \mathbf{y}_P^{(j)}} = \underbrace{\mathbf{F}_M \bar{\mathbf{H}}_P^{(j)} \mathbf{F}_M^*}_{\triangleq \Lambda_P^{(j)}} \mathbf{x} + \mathbf{F}_M \bar{\mathbf{i}}_P^{(j)} + \underbrace{\mathbf{F}_M \bar{\mathbf{n}}_P^{(j)}}_{\triangleq \mathbf{n}_P^{(j)}}, \tag{4}$$

[1] This is a worst-case assumption since spatial correlation between the outputs of the PLC and/or wireless system can be exploited to further mitigate IN and NBI effects; see, e.g., [13] for an example from DSL systems.

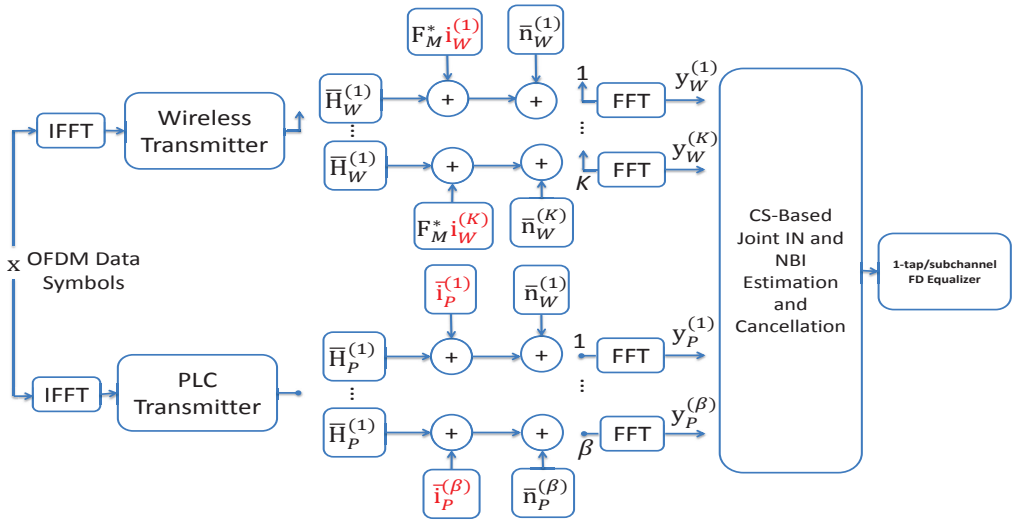

Fig. 1. A block diagram of the system model of a SIMO hybrid wireless/PLC system. For simplicity, the CFO and windowing are not shown in this figure, i.e., $\Phi = \mathbf{D}_W^{(k)} = \mathbf{I}_M$. Here, red fonts are used to indicate sparse vectors.

where Φ is an $M \times M$ diagonal matrix whose diagonal elements are the window coefficients. We use the Hamming window as an example to quantify the effects of windowing on NBI sparsity. Moreover, the matrices $\Lambda_W^{(k)}$ and $\Lambda_P^{(j)}$ denote the $M \times M$ effective channel matrices. Here, $\mathbf{i}_W^{(k)}$ denotes the frequency-domain (FD) NBI vector at the k^{th} antenna.

Concatenating the received wireless and PLC signals in (3) and (4) for all $k \in \{1, \ldots, K\}$ and $j \in \{1, \ldots, \beta\}$ into a single column vector results in

$$\underbrace{\begin{bmatrix} \mathbf{y}_W^{(1)} \\ \vdots \\ \mathbf{y}_W^{(K)} \\ \mathbf{y}_P^{(1)} \\ \vdots \\ \mathbf{y}_P^{(\beta)} \end{bmatrix}}_{\triangleq \mathbf{y}} = \underbrace{\begin{bmatrix} \Lambda_W^{(1)} \\ \vdots \\ \Lambda_W^{(K)} \\ \Lambda_P^{(1)} \\ \vdots \\ \Lambda_P^{(\beta)} \end{bmatrix}}_{\triangleq \mathbf{G}} \mathbf{x} + \underbrace{\begin{bmatrix} \mathbf{i}_W^{(1)} \\ \vdots \\ \mathbf{i}_W^{(k)} \\ \mathbf{F}_M \bar{\mathbf{i}}_P^{(1)} \\ \vdots \\ \mathbf{F}_M \bar{\mathbf{i}}_P^{(\beta)} \end{bmatrix}}_{\triangleq \mathbf{i}} + \underbrace{\begin{bmatrix} \mathbf{n}_W^{(1)} \\ \vdots \\ \mathbf{n}_W^{(K)} \\ \mathbf{n}_P^{(1)} \\ \vdots \\ \mathbf{n}_P^{(\beta)} \end{bmatrix}}_{\triangleq \mathbf{n}}. \quad (5)$$

We term the $M(K+\beta)\times 1$ vector $\mathbf{y}$ as the *measurement vector*, while the $M(K+\beta)\times M$ matrix $\mathbf{G}$ is termed the *measurement matrix*. Finally, $\mathbf{i}$ denotes the combined $M(K+\beta)\times 1$ NBI and IN vectors, while $\mathbf{n}$ is the equivalent $M(K+\beta)\times 1$ FD noise vector. Our main goal in this paper is to use (5) for accurate estimation of the NBI and IN vectors.

III. CS-Based Joint NBI and IN Estimation

To estimate the NBI and IN vectors from $\mathbf{y}$, we first cancel the unknown term $\mathbf{Gx}$ in (5) by projecting $\mathbf{y}$ onto the left-null space of $\mathbf{G}$ using the following projection matrix [5], [10]: $\mathbf{Q} = \mathbf{I}_{M(K+\beta)} - \mathbf{G}\mathbf{G}^{\dagger}$, where $\mathbf{G}^{\dagger}$ denotes the Moore-Penrose pseudo-inverse of $\mathbf{G}$ that is given by $\left(\mathbf{G}^H\mathbf{G}\right)^{-1}\mathbf{G}^H$ for the case of a full-column-rank $\mathbf{G}$. Since $\mathbf{QG} = \mathbf{0}_{M(K+\beta)\times M}$, we obtain the following expression after this projection step:

$$\mathbf{y}' \triangleq \mathbf{Q}\mathbf{y} = \mathbf{Q}\mathbf{i} + \mathbf{Q}\mathbf{n} \triangleq \mathbf{Q}_{\text{eqn}}\mathbf{i}_{\text{eqn}} + \mathbf{n}'. \quad (6)$$

Here, $\mathbf{i}_{\text{eqn}} \triangleq \begin{bmatrix} \mathbf{i}_W^{(1)^T} & \ldots & \mathbf{i}_W^{(K)^T} & \bar{\mathbf{i}}_P^{(1)^T} & \ldots & \bar{\mathbf{i}}_P^{(\beta)^T} \end{bmatrix}^T$, $\mathbf{n}' \triangleq \mathbf{Q}\mathbf{n}$, and the *modified measurement matrix* $\mathbf{Q}_{\text{eqn}}$ is defined in terms of $\mathbf{Q}$ as follows

$$\mathbf{Q}_{\text{eqn}} = \mathbf{Q}\underbrace{\begin{bmatrix} \mathbf{I}_{KM} & \mathbf{0}_{KM\times\beta M} \\ \mathbf{0}_{\beta M\times KM} & \mathbf{I}_\beta \otimes \mathbf{F}_M \end{bmatrix}}_{\triangleq \mathbf{A}}, \quad (7)$$

where $\otimes$ denotes the Kronecker product operation.

A. NBI and IN estimation in the presence of NBI CFO

In this section, we investigate reconstructing $\mathbf{i}_{\text{eqn}}$ in the presence of NBI CFO without assuming block-sparse structure for the NBI or IN vectors. Based on the linear model in (6), $\mathbf{i}_{\text{eqn}}$ can be estimated by solving the following l_1-norm convex optimization problem that can be solved using convex optimization techniques:

$$\hat{\mathbf{i}}_{\text{eqn}} \triangleq \underset{\mathbf{i}\in\mathbb{C}^{(K+\beta)M}}{\text{argmin}} \|\mathbf{i}\|_1 \quad \text{subject to} \quad \|\mathbf{Q}_{\text{eqn}}\mathbf{i} - \mathbf{y}'\|_2^2 \le \epsilon_1, \quad (8)$$

where ϵ_1 is set such that $\epsilon_1 \le \|\mathbf{n}'\|_2^2$ with high probability. To further improve the $\mathbf{i}_{\text{eqn}}$ estimate, we introduce an additional constraint, based on (5), to formulate the following convex optimization problem

$$\hat{\mathbf{i}}_{\text{eqn}} \triangleq \underset{\mathbf{i}\in\mathbb{C}^{(K+\beta)M}}{\text{argmin}} \|\mathbf{i}\|_1$$
$$\text{subject to} \quad (9)$$
$$\|\mathbf{y}' - \mathbf{Q}_{\text{eqn}}\mathbf{i}\|_2^2 \le \epsilon_1 \quad \text{and} \quad \|\mathbf{y} - \mathbf{A}\mathbf{i}\|_2^2 \le \epsilon_2,$$

where $\mathbf{A}$ is defined in (7) and ϵ_2 is a quantity that can upper bound $\|\mathbf{Gx} + \mathbf{n}\|_2^2$ with high probability. We use $\hat{\mathbf{i}}_{\text{eqn}}$ to find the support of $\mathbf{i}_{\text{eqn}}$ as follows [11]:

$$I = \left\{ j : \left|\hat{\mathbf{i}}[j]_{\text{eqn}}\right|^2 > \frac{\max\{\epsilon_1, \epsilon_2\}}{(K+\beta)M} \right\}, \quad (10)$$

where $\hat{\mathbf{i}}[j]_{\text{eqn}}$ is the j^{th} element of the vector $\hat{\mathbf{i}}_{\text{eqn}}$.

B. Joint NBI-IN estimation assuming known bursts boundaries

Both NBI and IN can be modeled as block sparse vectors that are constructed from few non-zero blocks where each block consists of d_W and d_P elements, respectively. Hence,

$\mathbf{i}_W^{(k)}$ and $\bar{\mathbf{i}}_P^{(j)}$ can be decomposed into ζ_x blocks, where $\zeta_x = \frac{M}{d_x}$ and $x \in \{W,\ P\}$ assuming that the number of sub-carriers M is an integer multiple of the block size d_x. These blocks are denoted by $\mathbf{i}_W^{(k)}[u_W]$ and $\bar{\mathbf{i}}_P^{(j)}[u_P]$, respectively, where $u_x \in \{1 \cdots \zeta_x\}$, and can be written as follows:

$$\mathbf{i}_W^{(k)} = [\underbrace{i_{W,1}^{(k)} \cdots i_{W,d_W}^{(k)}}_{\left(\mathbf{i}_W^{(k)}[1]\right)^T} \cdots \underbrace{i_{W,M-d_W+1}^{(k)} \cdots i_{W,M}^{(k)}}_{\left(\mathbf{i}_W^{(k)}[\zeta_W]\right)^T}]^T, \quad (11)$$

$$\bar{\mathbf{i}}_P^{(j)} = [\underbrace{\bar{i}_{P,1}^{(j)} \cdots \bar{i}_{P,d_P}^{(j)}}_{\left(\bar{\mathbf{i}}_P^{(j)}[1]\right)^T} \cdots \underbrace{\bar{i}_{P,M-d_P+1}^{(j)} \cdots \bar{i}_{P,M}^{(j)}}_{\left(\bar{\mathbf{i}}_P^{(j)}[\zeta_P]\right)^T}] \cdot T \quad (12)$$

In particular, $\mathbf{i}_W^{(k)}$ and $\bar{\mathbf{i}}_P^{(j)}$ are called block-sparse vectors and $\rho_W^{(k)} \triangleq \sum_{j=1}^{\zeta_W} \mathbf{1}\left\{\|\mathbf{i}_W^{(k)}[j]\|_2\right\}$ and $\rho_P^{(j)} \triangleq \sum_{l=1}^{\zeta_P} \mathbf{1}\left\{\|\mathbf{i}_W^{(k)}[l]\|_2\right\}$ count the number of nonzero blocks, respectively. The indicator function $\mathbf{1}\{.\}$ is equal to 1 for non-zero argument and 0 otherwise. For $d_W = d_P = 1$, $\rho_W^{(k)}$ and $\rho_P^{(j)}$ counts the number of non-zero entries in $\mathbf{i}_W^{(k)}$ and $\bar{\mathbf{i}}_P^{(j)}$, respectively.

This reduces the problem of NBI and IN estimation to estimation of an S-block sparse vector $\mathbf{i}_{\text{eqn}}$, where $S \triangleq \sum_{k=1}^{K} \rho_W^{(k)} + \sum_{j=1}^{\beta} \rho_P^{(j)}$. Exploiting this block sparse structure of $\mathbf{i}_{\text{eqn}}$, we estimate $\mathbf{i}_{\text{eqn}}$ from (6) by solving the following optimization problem [7]:

$$\hat{\mathbf{i}}_{\text{eqn}} \triangleq \underset{\mathbf{i} \in \mathbb{C}^{(K+\beta)M}}{\operatorname{argmin}} \sum_{l=1}^{M(\frac{K}{d_W}+\frac{\beta}{d_P})} \|\mathbf{i}[l]\|_2 \quad \text{subject to} \quad \|\mathbf{Q}_{\text{eqn}}\mathbf{i} - \mathbf{y}'\|_2^2 \leqslant \epsilon. \quad (13)$$

Alternatively, a number of greedy algorithms in the CS literature can be used to solve this problem in an efficient manner. One of these algorithms is *block orthogonal matching pursuit* (BOMP) [7], which is an extension of the conventional OMP algorithm [14]. BOMP iteratively constructs the blocks of $\mathbf{i}_{\text{eqn}}$ by finding the block of the measurement matrix $\mathbf{Q}_{\text{eqn}}$ that is most correlated with measurements in (6) and then solving a least-squares problem using the selected blocks[2]. These blocks are constructed from the column vectors of $\mathbf{Q}_{\text{eqn}}$ and each one is of size $M(K+\beta) \times d$, where $d = \min\{d_W,\ d_P\}$, and defined as follows:

$$\mathbf{Q}_{\text{eqn}} = \quad (14)$$
$$[\underbrace{\mathbf{q}_{\text{eqn},1} \cdots \mathbf{q}_{\text{eqn},d}}_{\mathbf{Q}_{\text{eqn}}[1]} \cdots \underbrace{\mathbf{q}_{\text{eqn},M(K+\beta)-d+1} \cdots \mathbf{q}_{\text{eqn},M(K+\beta)}}_{\mathbf{Q}_{\text{eqn}}[\frac{M(K+\beta)}{d}]}],$$

where $\mathbf{q}_{\text{eqn},u}$ denotes the u^{th} column of $\mathbf{Q}_{\text{eqn}}$. Below, we summarize main steps of the BOMP algorithm.

Inputs: Vector $\mathbf{y}'$, matrix $\mathbf{Q}_{\text{eqn}}$, and block sparsity level S.
Initialization: Define index set $I_0 = \{\}$, and set residual $\mathbf{r}_0 = \mathbf{y}'$, estimate $\hat{\mathbf{i}}_{\text{eqn}} = \mathbf{0}_{(K+\beta)M\times 1}$, and iteration count $l = 1$.
The l^{th} iteration:

1) Compute $\delta_i = \|\left(\mathbf{Q}_{\text{eqn}}[i]\right)^H \mathbf{r}_{l-1}\|_2$ for all $i \notin I_{l-1}$.
2) Choose index of the next nonzero block computed during the l^{th} iteration as $c_l = \underset{i}{\operatorname{argmax}}\ \delta_i$.
3) Update the indices of nonzero blocks as $I_l = I_{l-1} \cup c_l$.
4) Solve the following optimization problem to obtain $\mathbf{i}_l[j]$ for $j \in I_l$:

$$\min_{\{\hat{\mathbf{i}}_l[j]\} \in I_l} \left\| \mathbf{y}' - \sum_{j \in I_l} \mathbf{Q}_{\text{eqn}}[j]\hat{\mathbf{i}}_l[j] \right\|_2. \quad (15)$$

5) Compute the residual error term in the l^{th} iteration as

$$\mathbf{r}_l = \mathbf{y}' - \sum_{j \in I_l} \mathbf{Q}_{\text{eqn}}[j]\mathbf{i}_l[j]. \quad (16)$$

6) If $l = S$ then exit, else set $l = l + 1$ and go to Step 1.

Note that even if d is equal to the size of the nonzero blocks in $\mathbf{i}_{\text{eqn}}$ and the boundaries of those blocks are not known, then the BOMP performance can be severely degraded since the modified measurement matrix $\mathbf{Q}_{\text{eqn}}$ can not be divided into sub-matrices that perfectly align with the blocks of $\mathbf{i}_{\text{eqn}}$. This challenge is addressed in the next section.

C. Joint NBI-IN estimation with unknown bursts' boundaries

In this section, we relax the known bursts' block boundaries assumption in Section III-B, i.e., the nonzero blocks of $\mathbf{i}_{\text{eqn}}$ may not align with the $\mathbf{Q}_{\text{eqn}}$ predefined sub-matrices in (14). Only the number of nonzero entries, denoted by W, and the number of clusters (bursts), denoted by C, are assumed known.

In [8], a new CS recovery algorithm, called the (W, C) algorithm, was proposed. This algorithm exploits the block sparse structure with no prior knowledge on the block boundary location, i.e., only knowledge of W and C is required. Moreover, this so-called (W, C) algorithm is based on the compressive sampling matching pursuit (CoSaMP) algorithm [15] with modified pruning based on dynamic programming principles. For completeness, we summarize the main steps of the (W, C) algorithm below.

Inputs: Vector $\mathbf{y}'$, matrix $\mathbf{Q}_{\text{eqn}}$, number of nonzero entries W, block sparsity level C and the normalized difference between estimated vector in two consecutive iterations denoted by μ.
Initialization: Set residual $\mathbf{r}_0 = \mathbf{y}'$, estimate $\hat{\mathbf{i}}_{\text{eqn},0} = \mathbf{0}_{(K+\beta)M\times 1}$, and iteration count $l = 1$.
The l^{th} iteration:

1) Update the residual as $\mathbf{r}_l = \mathbf{y}' - \mathbf{Q}_{\text{eqn}}\hat{\mathbf{i}}_{\text{eqn},l-1}$.
2) Compute $\mathbf{e} = \mathbf{Q}_{\text{eqn}}^H \mathbf{r}_l$.
3) Prune $\mathbf{e}$ using $|\mathbf{e}|$ to find the best $2W$ indices set $\mathbf{\Omega}$ for $2C$ clusters based on the pruning algorithm in [8].
4) Construct set $T = \mathbf{\Omega} \cup \text{supp}\left(\hat{\mathbf{i}}_{\text{eqn},l-1}\right)$, where $\text{supp}\,(\mathbf{x})$ denotes indices of the nonzero entries of $\mathbf{x}$.
5) Define $\mathbf{b} = \mathbf{0}_{(K+\beta)M\times 1}$ and estimate the entries belonging to the set T by applying least square (LS) as follows: $\mathbf{b}|_T = \mathbf{Q}_{\text{eqn}}(:, T)^{\dagger}\mathbf{y}'$, where $\mathbf{Q}_{\text{eqn}}(:, T)$ is constructed from the $\mathbf{Q}_{\text{eqn}}$ columns indexed by T.
6) Prune $\mathbf{b}$ using the absolute values $|\mathbf{b}|$ to find the best W nonzero entries in C clusters and obtain $\hat{\mathbf{i}}_{\text{eqn},l}$.
7) The stopping criterion depends on the convergence of the estimated $\hat{\mathbf{i}}_{\text{eqn},l}$. If $\frac{\|\hat{\mathbf{i}}_{\text{eqn},l} - \hat{\mathbf{i}}_{\text{eqn},l-1}\|}{\|\hat{\mathbf{i}}_{\text{eqn},l}\|} \leq \mu$, where μ captures

[2]Most of sparse-block recovery algorithms, including BOMP, assume that blocks' boundaries are known apriori in order to construct the measurement matrix blocks [7]. However, this assumption may not be satisfied in our problem, which results in poor performance as will be shown in Section IV.

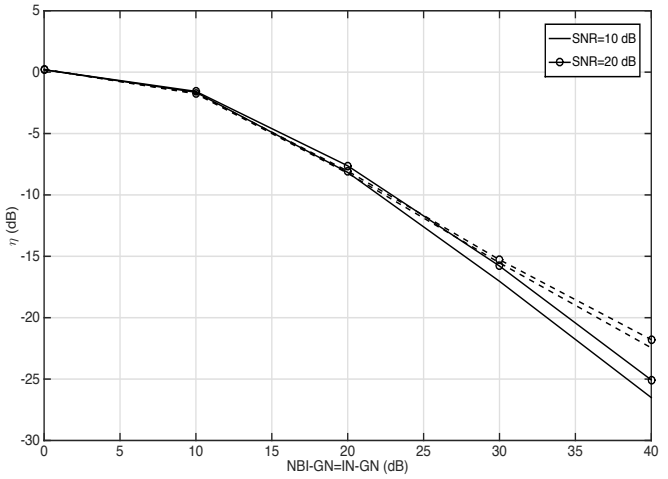

Fig. 2. AEVM versus IN-GN=NBI-GN with width=3 IN and NBI at each wire and recieve antenna, respectively, i.e. $d = 3$. NBI and IN are estimated using the CS recovery algorithm in Section III-A. Dashed and solid curves represent results without and with windowing, respectively.

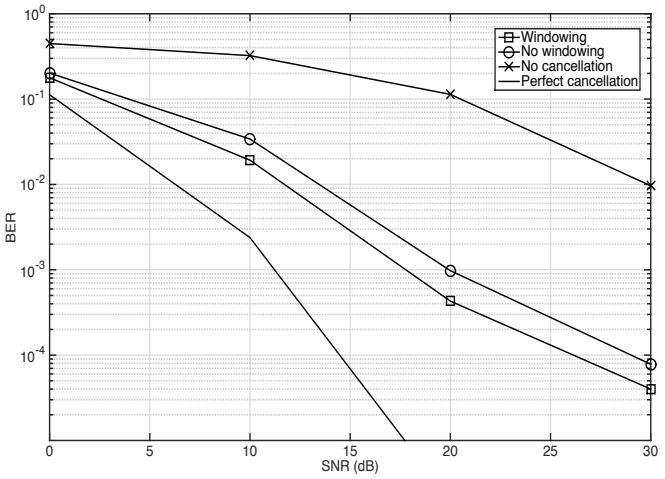

Fig. 3. BER performance versus SNR for $R = 4$ bits/sec/Hz and NBI-GN=IN-GN=40 dB using the CS recovery algorithm in Section III-A.

the performance-complexity trade-off (the smaller μ is, the better estimate can be obtained with more iterations), then exit, else set $l = l + 1$ and go to Step 1.

The key idea of the new pruning algorithm proposed in [8] is to apply dynamic programming principles to iteratively construct the clusters. In each pruning iteration, either new elements are added to the already constructed clusters, or those clusters are split into more clusters until all of the W nonzero entries in the C clusters are computed. We refer the reader to [8] for more details on the pruning algorithm.

IV. Numerical Results

In this section, we report the results of our numerical experiments to evaluate the performance of our investigated CS-based schemes for joint mitigation of NBI and IN in hybrid PLC-wireless systems. Our simulation environment corresponds to $K = 3, \beta = 3$ and $M = 64$, unless otherwise mentioned. For the wireless channel modeling, we assume a uniform power delay profile with $L_W = 8$ zero-mean complex Gaussian CIR taps with normalized powers; i.e., $\mathbb{E}\big[|\bar{\mathbf{h}}_W^{(k)H}\bar{\mathbf{h}}_W^{(k)}|^2\big] = 1,\ k \in \{1,2,3\}$. We also assume that the receive antennas suffer from independent contiguous narrowband interferers that occupy independent subcarrier indices and whose amplitudes are independent zero-mean complex Gaussian taps with fixed NBI-to-background Gaussian noise (NBI-GN) ratio, defined as $\frac{\mathbb{E}\left[\mathbf{i}_W^{(k)H}\mathbf{i}_W^{(k)}\right]}{\sigma_W^2},\ \forall\ k \in \{1,2,3\}$. Unless otherwise stated, we assume that each narrowband interferer has a fixed width of 3 contiguous sub-carriers. This setup is similar to a Bluetooth signal (with 1 MHz bandwidth) interfering with an IEEE 802.11 g/n signal (with 20 MHz bandwidth) [16], and is of high practical interest due to collocated Bluetooth and WLAN signals in the unlicensed 2.4 GHz frequency band.

We assume that each PLC channel consists of two equal-power taps, i.e., $L_p = 2$, having uniformly-distributed phases and lognormal-distributed magnitudes with standard deviations of 0.6 [2], [17]. We assume unit-power channels; i.e. $\mathbb{E}\big[|\bar{\mathbf{h}}_P^{(j)H}\bar{\mathbf{h}}_P^{(j)}|^2\big] = 1,\ \forall\ j \in \{1,2,3\}$ and we assume that the IN is spread over 3 contiguous time samples. Finally, we assume a fixed IN-to-background Gaussian noise (IN-GN) ratio, defined as $\frac{\mathbb{E}\left[\bar{\mathbf{i}}_P^{(j)H}\bar{\mathbf{i}}_P^{(j)}\right]}{\sigma_P^2},\ j \in \{1,2,3\}$.

To quantify the performance of all investigated CS recovery schemes in terms of NBI and IN estimation accuracy, we use the performance metric of *average error vector magnitude* (AEVM), which we define as $\eta \triangleq \frac{\sum_{u=1}^{U}\|\mathbf{i}_{\text{eqn}}-\hat{\mathbf{i}}_{\text{eqn}}\|_2^2}{\sum_{u=1}^{U}\|\mathbf{i}_{\text{eqn}}\|_2^2}$ with U denoting the number of channel realizations. Note that a smaller value of η indicates better estimation performance.

In Fig. 2, we investigate the effect of applying time-domain windowing in the presence of asynchronous NBI with uniformly-distributed CFO as defined in Section II. Moreover, we set NBI-GN=IN-GN, both the NBI and IN clusters are assumed to have the same width of 3, and we use the CS recovery algorithm in Section III-A. As shown in Fig. 2, the weaker the desired signal is, the higher the gain of using windowing since the NBI effect becomes more detrimental. Similar conclusions can be drawn from the BER simulations in Fig. 3, which show up to 3 dB gain at BER = 5×10^{-4} due to windowing.

To investigate the performance of the block-sparse recovery algorithms, we set the number of PLC and wireless outputs to $K = \beta = 1$ to separate the effect of any gain due to processing of multiple outputs. In Fig. 4, we use the metric η to compare between the performances of the OMP, BOMP, and (W, C) algorithms. As a performance lower bound, we plot the (ideal) LS performance assuming that the locations of the nonzero entries are perfectly known. The NBI and IN clusters are assumed to be of the same width of 5 and can lie anywhere within the OFDM symbol, i.e., locations of the burst boundaries are not known. For BOMP, there is a mismatch between the clusters' boundaries and the predefined sub-matrices of $\mathbf{Q}_{\text{eqn}}$ in (14). As shown in Fig. 4, the performance of BOMP is severely degraded compared with that of the OMP and (W,C) algorithms and this degradation becomes more severe as the IN-GN level increases. In addition, the (W, C) algorithm outperforms the conventional OMP algorithm over the whole IN-GN range. At high IN-GN levels, the performance gap between the (W, C) and conventional OMP diminishes since the higher powers of the NBI and IN signals (relative to the thermal noise level) enable accurate sparse recovery for both

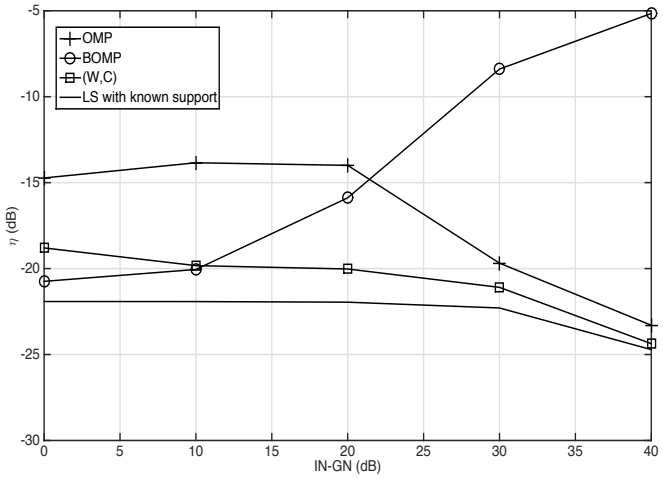

Fig. 4. AEVM versus IN-GN with NBI-GN=40dB for SISO systems. Here, NBI and IN clusters are assumed to be of width 5.

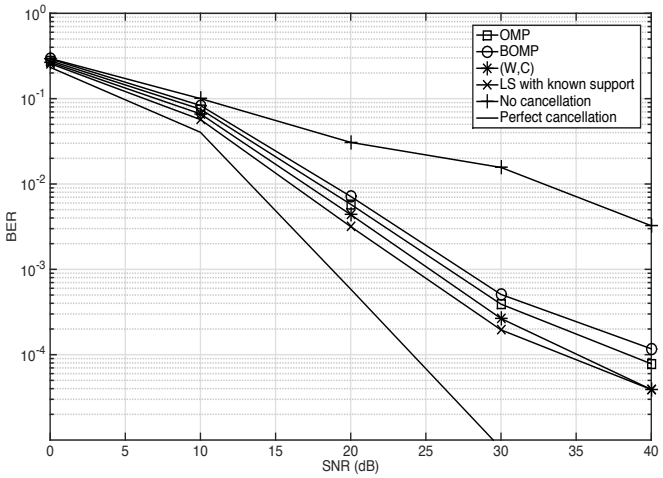

Fig. 5. BER performance versus SNR for $R = 4$ bits/sec/Hz, NBI-GN=40dB and IN-GN=20dB. Both NBI and IN have the same width of 5.

algorithms without the need for exploiting their bursty nature. Moreover, both algorithms approach the ideal LS lower bound.

To further illustrate the performance gain achieved by exploiting the block-sparse structure, Fig. 5 compares the BER of the aforementioned joint NBI/IN estimation algorithms. The (W, C) algorithm achieves more than 2dB and 5dB SNR gain at BER=10^{-4} over the conventional OMP and BOMP algorithms, respectively. Moreover, as SNR increases, the (W, C) algorithm approaches the LS performance with perfect NBI and IN location knowledge. Finally, Fig. 6 shows the BER performance, for a more general scenario, when the NBI and IN clusters have different widths of 3 and 5, respectively. In this scenario, the performance gain of the (W, C) algorithm over the BOMP algorithm increases compared to the equal width scenario in Fig. 5. For example, at BER =10^{-3}, an SNR gain of 5dB is achieved while only a gain of 2.5dB is achieved when the NBI and IN clusters have the same width.

V. Conclusions

In this paper, we proposed joint processing of the hybrid wireless and PLC systems outputs to jointly suppress NBI and IN by exploiting their sparsity in the frequency and time domains, respectively. Moreover, we generalized our model to accommodate the practical scenario of asynchronous NBI and investigated the application of time-domain windowing

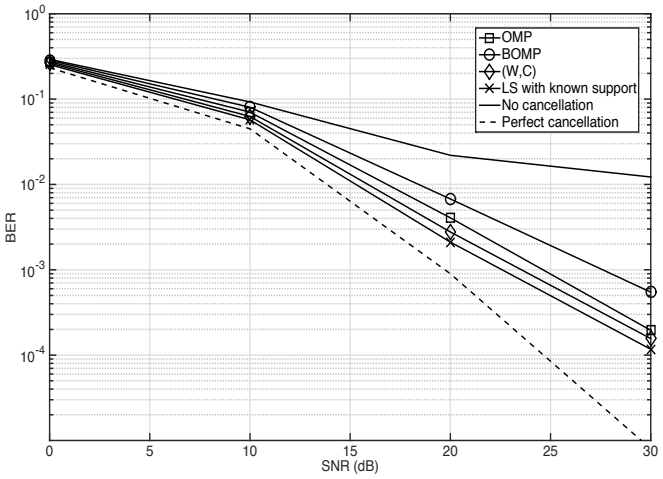

Fig. 6. BER performance versus SNR for $R = 4$ bits/sec/Hz, NBI-GN=40dB and IN-GN=20dB, with NBI and IN widths of 3 and 5, respectively.

to enhance the NBI sparsity and, hence, CS-based estimation of the NBI signal. Furthermore, we designed joint IN and NBI mitigation schemes to exploit their inherent block sparsity (bursty nature) with and without knowledge of the bursts' boundaries. Finally, we quantified the performance gains of our proposed schemes through extensive numerical simulations.

References

[1] J. G. Proakis, *Digital Communication*, 4th ed. McGraw-Hill, 2001.

[2] S. Guzelgoz, H. Celebi, and H. Arslan, "Analysis of a MultiChannel Receiver: Wireless and PLC Reception," in *Proc. EUSIPCO*, Aug. 2010.

[3] S. Lai and G. Messier, "Using the Wireless and PLC Channels for Diversity," *IEEE Trans. Commun.*, pp. 3865–3875, Dec 2012.

[4] V. Oksman and J. Zhang, "G.HNEM: The New ITU-T Standard on Narrowband PLC Technology," *IEEE Comm. Mag.*, Dec. 2011.

[5] A. Gomaa and N. Al-Dhahir, "A Sparsity-Aware Approach for NBI Estimation in MIMO-OFDM," *IEEE Trans. Wireless Comm.*, Jun. 2011.

[6] H. Ferreira, L. Lampe, J. Newbury, and T. Swart, *Power Line Communications: Theory and Applications for Narrowband and Broadband Communications over Power Lines*. John Wiley & Sons, 2010.

[7] Y. Eldar, P. Kuppinger, and H. Bolcskei, "Block-Sparse Signals: Uncertainty Relations and Efficient Recovery," *IEEE Transactions on Signal Processing*, vol. 58, no. 6, pp. 3042–3054, June 2010.

[8] V. Cevher, P. Indyk, C. Hegde, and R. G. Baraniuk, "Recovery of Clustered Sparse Signals from Compressive Measurements ," in *Proc. Int. Conf. Sampling Theory Applicat. (SAMPTA), May 2009*.

[9] E. Candes, J. Romberg, and T. Tao, "Stable Signal Recovery from Incomplete and Inaccurate Measurements," *Comm. Pure App. Math.*, vol. 59, no. 9, pp. 1207–1223, Mar 2006.

[10] G. Caire, T. Al-Naffouri, and A. Narayanan, "Impulse Noise Cancellation in OFDM: An Application of Compressed Sensing," in *Proc. IEEE Intl. Symp. Information Theory (ISIT)*, Jul. 2008, pp. 1293–1297.

[11] L. Lampe, "Bursty Impulse Noise Detection by Compressed Sensing," in *IEEE International Symposium on Power Line Communications and Its Applications (ISPLC), 2011*, April 2011, pp. 29–34.

[12] M. Mokhtar, W. Bajwa, and N. Al-Dhahir, "Sparsity-Aware Joint Narrowband Interference and Impulse Noise Mitigation for Hybrid Powerline-Wireless Transmission," in *Proc. IEEE Wireless Communications and Networking Conference (WCNC), March 2013* .

[13] A. Awasthi, N. Al-Dhahir, O. Eliezer, and P. Balsara, "Alien Crosstalk Mitigation in Vectored DSL Systems for Backhaul Applications," in *Proc. IEEE Intl. Conf. Commun. (ICC)*, Jun. 2012, pp. 3852–3856.

[14] Y. Pati, R. Rezaiifar, and P. Krishnaprasad, "Orthogonal Matching Pursuit: Recursive Function Approximation with Applications to Wavelet Decomposition," in *Proc. Asilomar Conf. Sig., Syst. and Comp.*, 1993.

[15] D. Needell and J. Tropp, "CoSaMP: Iteative Signal Recovery from Incomplete and Inaccurate Samples," *Appl. Computat. Harmon. Anal.*, vol. 26, no. 3, pp. 301–321, May 2009.

[16] E. Perahia and R. Stacey, *Next Generation Wireless LANs*. Cambridge University Press, 2013.

[17] S. Galli, "A Novel Approach to the Statistical Modeling of Wireline Channels," *IEEE Trans. Commun.*, pp. 1332–1345, May 2011.